

Anisotropic spin waves in a metallic antiferromagnet $\text{Nd}_{0.45}\text{Sr}_{0.55}\text{MnO}_3$

H. Yoshizawa

Neutron Scattering Laboratory, I. S. S. P., University of Tokyo, Tokai, Ibaraki 319-1106, Japan

H. Kawano

The Institute of Physical and Chemical Research (RIKEN), Wako, Saitama 351-01, Japan

J. A. Fernandez-Baca

Solid State Division, Oak Ridge National Laboratory, Oak Ridge, Tennessee 37831

H. Kuwahara

Joint Research Center for Atom Technology (JRCAT), Tsukuba, Ibaraki 305, Japan

Y. Tokura

*Joint Research Center for Atom Technology (JRCAT), Tsukuba, Ibaraki 305, Japan
and Department of Applied Physics, University of Tokyo, Bunkyo-ku, Tokyo 113, Japan*

(Received 11 February 1998)

We demonstrate that $\text{Nd}_{0.45}\text{Sr}_{0.55}\text{MnO}_3$ is an example of a metallic antiferromagnetic manganite, and that it exhibits very anisotropic spin-wave dispersion relations with intra- and interplanar exchange parameters $8JS = 32.6 \pm 0.9$ meV and $4J'S = -10.1 \pm 0.5$ meV, respectively. This anisotropy reflects underlying $d_{x^2-y^2}$ -type orbital ordering, and the metallic behavior indicates that a charge ordering is decoupled from the orbital ordering in this system. [S0163-1829(98)51926-1]

Recent experimental studies on colossal magnetoresistance (CMR) phenomena in perovskite manganites demonstrate that the melting of the charge ordering can have a drastic influence on the change of the resistivity at the insulator to metal transition. For example, a so-called CE-type charge ordering is formed in a system with the hole concentration of a commensurate value $n_h \sim 1/2$, but an external magnetic field of a few Tesla can trigger extraordinary CMR effects in $\text{Pr}_{1-x}\text{Ca}_x\text{MnO}_3$ (Refs. 1 and 2) and $\text{Nd}_{1/2}\text{Sr}_{1/2}\text{MnO}_3$.³

Very recently, on the other hand, we have studied three manganites with $n_h \sim 1/2$, and demonstrated that, instead of the well-known CE-type magnetic structure, some manganites may have a layered A-type antiferromagnetic (AFM) ordering, in which the ferromagnetic layers stack antiferromagnetically.⁴ The change of the magnetic structure from a CE-type to an A-type can be interpreted as an effect of widening of the one-electron bandwidth. The behavior of the resistivity of the A-type manganites is also distinctly different from those with the CE-type orbital and spin ordering. Based on the detailed study of the lattice and spin structure of the A-type manganites, we further suggested the possibility of the *two-dimensional* character in both magnetic and transport properties.⁴ Here, it should be noted that throughout this paper we employ a terminology of the *two-dimensional character* to emphasize a layered-type large anisotropy in the physical properties which results from the underlying orbital ordering in an A-type manganite.

To examine such a possibility in magnetism, we performed a detailed study of its spin dynamics. For this study, we chose $\text{Nd}_{0.45}\text{Sr}_{0.55}\text{MnO}_3$ as an example of the A-type AFM compounds near $n_h \sim 1/2$. In the present paper, we

shall demonstrate that $\text{Nd}_{0.45}\text{Sr}_{0.55}\text{MnO}_3$ is the first example of a *metallic AFM* manganite, by showing that the temperature dependence of the resistivity of this sample is metallic even below T_N . In addition, the spin-wave dispersion relation of $\text{Nd}_{0.45}\text{Sr}_{0.55}\text{MnO}_3$, indeed, possesses a “*quasi*”-*two-dimensional character*, and this can be understood as the result of the underlying orbital ordering. These results imply that the charge ordering is decoupled with the orbital ordering in the present system. Furthermore, we shall report that the spin fluctuations in the paramagnetic phase of the A-type $\text{Nd}_{0.45}\text{Sr}_{0.55}\text{MnO}_3$ are dominated by the ferromagnetic (FM) spin fluctuations.

Most of the neutron-scattering measurements were performed with triple axis spectrometers at the High Flux Isotope Reactor in Oak Ridge National Laboratory. The spectrometers were operated with either $E_f = 30.5$ or 13.7 meV with a combination of $50'$ - $40'$ - $60'$ - $60'$ collimators. For the scans which require the better energy resolution, we employed a spectrometer installed at the cold guide tube in the JRR-3M reactor in Tokai, Japan. An incident momentum of $k_i = 1.55 \text{ \AA}^{-1}$ with open- $80'$ - $80'$ collimators from monochromator to detector yielded an energy resolution of ~ 0.23 meV (full width at half maximum). Samples were shielded in an aluminum capsule with exchange helium gas, and mounted at the cold head of a closed-cycle He-gas refrigerator. The sample temperature was controlled within accuracy of 0.2° or better.

A detailed procedure of the sample preparation was reported in preceding papers.^{3,4} The Sr concentration and oxygen contents were evaluated with standard procedures,^{3,4} and the results showed that the hole concentration agrees with a nominal concentration within 1% accuracy.

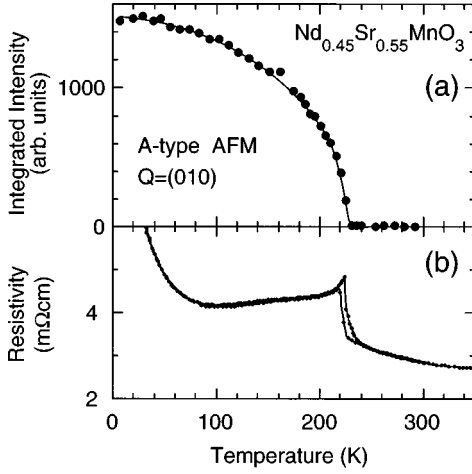


FIG. 1. Temperature dependence of AFM Bragg reflection at $Q=(010)$ and the resistivity in $\text{Nd}_{0.45}\text{Sr}_{0.55}\text{MnO}_3$.

$\text{Nd}_{0.45}\text{Sr}_{0.55}\text{MnO}_3$ has the orthorhombic $Pnma$ structure with lattice parameters, $a=5.360 \text{ \AA}$, $b/\sqrt{2}=5.498 \text{ \AA}$, and $c=5.413 \text{ \AA}$ at 250 K. The single crystal sample was aligned with the $(h|h)$ scattering plane. The spin-wave profiles were observed around the A-type AFM Bragg points, $Q=(111)$ and (010) , while the FM spin fluctuations were observed around the nuclear Bragg reflection $Q=(101)$.

Figure 1 shows the temperature dependence of the A-type AFM Bragg intensity and that of the resistivity, respectively. At low temperatures below $T_N \sim 225 \text{ K}$, the system shows an A-type AFM order in which ferromagnetic layers stack antiferromagnetically, and the A-type AFM Bragg reflections appear in appropriate Q positions as exemplified by the (010) reflection in Fig. 1(a). At T_N the resistivity shows a sharp jump, but it becomes metallic below T_N until $T \sim 80 \text{ K}$, as shown in Fig. 1(b). The metallic behavior of the resistivity below T_N implies that in this system a charge ordering is unlikely to be formed below T_N . The step and the hysteresis in the resistivity observed at T_N is simply due to the first-order structural phase transition.

At the magnetic phase transition $T_N \sim 225 \text{ K}$, this compound shows a simultaneous structural phase transition, where the crystal structure changes from an O^\dagger structure with $a < c < b/\sqrt{2}$ to an O' structure with $b/\sqrt{2} < a < c$ (not shown).⁴ Although the simultaneous structural phase transition is accompanied with hysteresis, indicating a first-order transition, the AFM phase transition is close to quasi second order, and allowed us to evaluate a critical index β of the magnetization. Our analysis yielded a value of β being $\sim 0.21 \pm 0.05$. This value indicates the *quasi-two-dimensional* character of magnetic properties in $\text{Nd}_{0.45}\text{Sr}_{0.55}\text{MnO}_3$, being consistent with our prediction.⁴

The quasi-two-dimensional character of $\text{Nd}_{0.45}\text{Sr}_{0.55}\text{MnO}_3$ is further evident in the spin dynamics. The AFM spin-wave excitations were observed at $\sim 12 \text{ K}$ along the directions parallel and perpendicular to the FM layers. Typical profiles observed at selected reduced wave vectors are illustrated in Figs. 2(a) and 2(b), where q_a and q_b denote the reduced wave vectors along the $[101]$ and $[010]$ directions, respectively. The additional intensity observed at $E \sim 17 \text{ meV}$ for $q_a=0.15$ in Fig. 2(a) is due to the crystal-field excitation from Nd ions. Note that $2q_a$ is close to q_b in units of \AA^{-1}

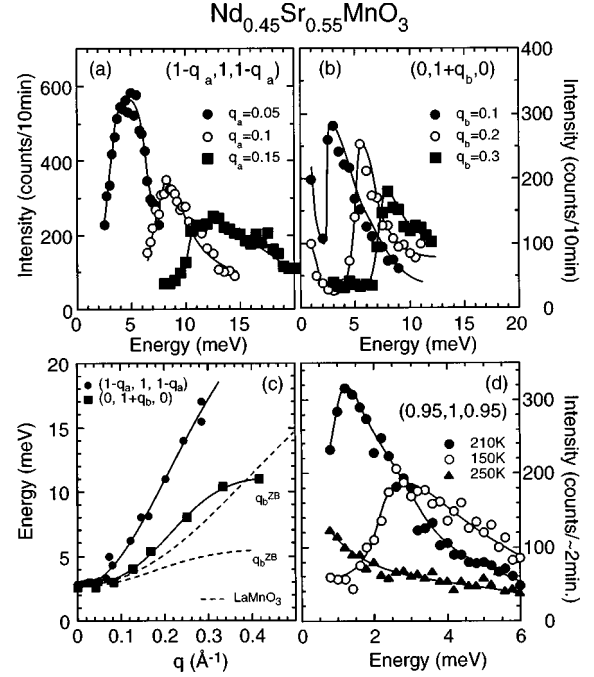


FIG. 2. (a) and (b) Spin-wave profiles at 12 K in $\text{Nd}_{0.45}\text{Sr}_{0.55}\text{MnO}_3$ measured at $Q=(1-q_a, 1, 1-q_a)$ and $(0, 1+q_b, 0)$ which correspond to the spin waves propagating within and perpendicular to the FM sheets in the A-type AFM, respectively. (c) Spin-wave dispersion in the A-type AFM $\text{Nd}_{0.45}\text{Sr}_{0.55}\text{MnO}_3$. Dashed curves indicate the dispersion relation of LaMnO_3 . Labels “ q_b^{ZB} ” indicate the zone boundary for the $[010]$ direction, while that for the $[101]$ direction is located at $q \sim 0.82 \text{ \AA}^{-1}$. (d) Spin-wave profiles observed at $Q=(0.95, 1, 0.95)$ at 210 K and 150 K $< T_N$, and 250 K $> T_N$.

due to a pseudocubic feature of the lattice constants. By comparing the profiles in Figs. 2(a) and 2(b), one can easily see that the spin waves propagating within the FM planes have higher spin-wave energy.

The obtained dispersion relations are depicted in Fig. 2(c), where a clear anisotropy of the excitation energy between the $[101]$ and $[010]$ directions indicates a *quasi-two-dimensional* feature of the magnetic properties. For comparison, the dispersion relations for the same two directions in LaMnO_3 which exhibits similar anisotropic spin waves⁵ are also depicted by dashed curves. To parametrize the dispersion relation, we adopted the same spin-wave dispersion formula which was employed for the analysis of LaMnO_3 in Ref. 5. For LaMnO_3 , the fit yielded $8JS = 13.36 \pm 0.18 \text{ meV}$, $4J'S = -4.84 \pm 0.22 \text{ meV}$, and $g\mu_B H_A = 0.61 \pm 0.11 \text{ meV}$, whereas for $\text{Nd}_{0.45}\text{Sr}_{0.55}\text{MnO}_3$, we obtained $8JS = 32.6 \pm 0.9 \text{ meV}$, $4J'S = -10.1 \pm 0.5 \text{ meV}$, and $g\mu_B H_A = 0.2 \pm 0.1 \text{ meV}$. These results indicate that the quasi-two-dimensional character of $\text{Nd}_{0.45}\text{Sr}_{0.55}\text{MnO}_3$ is about the same order with that of LaMnO_3 , although the exchange parameters in the present compound are roughly twice as large.

We have focused so far on the quasi-two-dimensional anisotropy of the spin-wave excitations in the low-temperature metallic AFM phase. We found, however, that the spin fluctuations in $\text{Nd}_{0.45}\text{Sr}_{0.55}\text{MnO}_3$ also show many other interesting behaviors as a function of temperature.

The temperature dependence of the spin-wave profiles was measured at selected q 's, and the typical results ob-

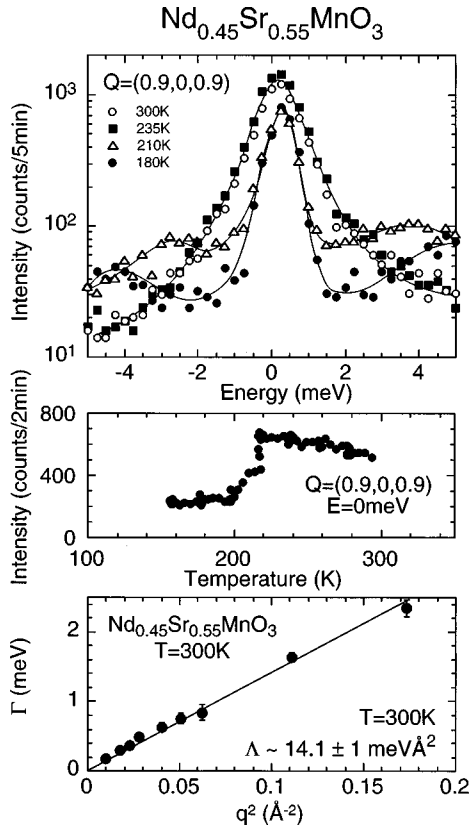


FIG. 3. (a) Ferromagnetic scattering observed above and below T_N in the A-type antiferromagnet $\text{Nd}_{0.45}\text{Sr}_{0.55}\text{MnO}_3$. (b) Temperature dependence of the ferromagnetic component observed at $Q = (1 + q_a, 0, 1 + q_a)$ with $q_a = -0.1$ and with $E = 0$ meV. (c) Wave-vector dependence of the energy width Γ of the ferromagnetic component observed at $T = 300$ K.

served at $Q = (0.95, 1, 0.95)$ are shown in Fig. 2(d). With increase of temperature, the AFM spin-wave energy gradually softens, and the AFM spin fluctuations vanish above T_N except for the tail of the incoherent scattering. Note that the pseudo-second-order character of the AFM phase transition is again manifested in the large softening of the spin-wave excitations towards T_N .

Corresponding to the disappearance of the AFM spin fluctuations above T_N , on the other hand, we find that the intense FM spin fluctuation appears in the paramagnetic phase at around the specific nuclear Bragg reflections. The temperature dependence of the FM component near T_N is summarized in Fig. 3. At the top panel, one can see that the diffusive FM spin fluctuation exists in the paramagnetic phase, but the evolution of the peak structure below T_N should be attributed to the AFM spin waves.

The middle panel shows that the diffusive FM component exhibits a sudden decrease below T_N , indicating that the major spectral weight of the spin fluctuations is transferred from the FM component in the paramagnetic phase to the AFM component below T_N . We would like to stress here that a similar switching in the spin fluctuations has been recently observed in some of the orbital- and charge-ordered manganites such as $\text{Pr}_{1-x}\text{Ca}_x\text{MnO}_3$ (Ref. 6) and $(\text{Bi,Ca})\text{MnO}_3$,⁷ and even in a vanadium oxide, V_2O_3 .⁸ For all these transition metal oxides, the orbital ordering is the crucial mechanism which triggers the switching of spin fluctua-

tions. These observations indicate that the switching of the spin fluctuations due to the orbital ordering is a rather common phenomenon in the transition-metal oxides with a freedom of the orbitals. The case of the present system is, however, very unique because the formation of the orbital ordering leads to the simultaneous magnetic and structural transitions at $T_N \sim 225$ K, but the charge ordering is not formed, and the resistivity remains metallic.

In the manganite systems, the type of orbital ordering may be easily identified since the orbital ordering is strongly correlated with the spin ordering and the lattice structure. In the $\text{Nd}_{1-x}\text{Sr}_x\text{MnO}_3$ system with $x \sim 1/2$, the lattice constants in the A-type AFM state satisfy the well-known relation of $b/\sqrt{2} < a < c$ for the O' structure,⁴ and consequently, the distance of the Mn ions between the ferromagnetic layers is shortest. Therefore, one expects that the e_g electrons occupy either the $d_{3x^2-r^2}$ - or the $d_{x^2-y^2}$ -type orbitals which lie within the FM layers. Since the manganites near $x \sim 1/2$ with the $d_{3x^2-r^2}$ -type orbitals exhibit the CE-type charge ordering, we expect the A-type spin structure to have the $d_{x^2-y^2}$ -type orbitals. The recent theoretical analyses favor our identification, in that they suggest that mobile holes in the manganites stabilize the $d_{x^2-y^2}$ -type orbital arrangement and the concomitant A-type spin structure around $x \sim 1/2$.⁹

One can expect very unique transport properties for this type of the orbital ordering. In this case, the matrix elements for the electron transfer between the FM layers are zero, and the resultant band for the e_g electrons is two-dimensional. The A-type spin structure with the double exchange (DE) mechanism further favors electron transfer within the FM layers, but discourages those between layers. Being consistent with these considerations, the resistivity in the A-type AFM state in $\text{Nd}_{0.45}\text{Sr}_{0.55}\text{MnO}_3$ is metallic, as shown in Fig. 1(b). In addition, clear anisotropic behavior of the resistivity has been recently observed in $\text{Nd}_{0.4}\text{Sr}_{0.6}\text{MnO}_3$.¹⁰

Finally, we found that the energy width of the observed FM component in the paramagnetic state is well described by the following equation, $\Gamma_q = \Lambda q^2$, and obtained $\Lambda \sim 14.1 \pm 1 \text{ meV}\text{\AA}^2$ as an effective spin-diffusion constant as shown at the bottom panel in Fig. 3. It should be noted that the effective spin-diffusion constant Λ is an order of magnitude smaller than the value of the spin stiffness constant $D_{SW} \sim 117 \text{ meV}\text{\AA}^2$ evaluated from the exchange parameters obtained in the present study. The results indicate that the onset of the AFM ordering in $\text{Nd}_{0.45}\text{Sr}_{0.55}\text{MnO}_3$ accompanies with the change of energy scale in spin fluctuations at the same time. The existence of the two energy scales in doped manganites is recently reported by thermopower and resistivity measurements.¹¹ The reported activation energy of the resistivity is close to the spin-wave stiffness constant D_{SW} obtained from the spin-wave dispersion in the low temperature AFM phase, whereas that of the thermopower is very close to the spin-diffusion constant Λ of the ferromagnetic spin fluctuations in the paramagnetic phase. The smaller energy scale for the low-energy ferromagnetic spin fluctuations in the paramagnetic state is presumably attributed to the hopping of the small polarons. When the Néel order is formed but the system remains *metallic*, the polaron-type spin fluctuations vanish from the system and the AFM fluctuations characterized by exchange parameters dominate.

We also note that the similar FM spin fluctuations are observed in the paramagnetic state of some of the hole-doped manganites with the hole concentration $n_h \sim 1/2$.^{6,12} For example, the FM diffusive component with the similar spin diffusion constant of $\Lambda \sim 15 \pm 2 \text{ meV \AA}^2$ was first reported in the FM metallic compound $\text{La}_{0.7}\text{Ca}_{0.3}\text{MnO}_3$,¹² and is also observed in the paramagnetic state of the CE-type charge ordered system $\text{Pr}_{1-x}\text{Ca}_x\text{MnO}_3$ with $0.35 \leq x \leq 0.50$.⁶ Therefore, with these results in mind, the present results corroborate the fact that a sharp FM central component exists in the paramagnetic state of the hole-doped manganites with a narrow one-electron band width *over a wide range of the hole concentration*, $0.3 \leq n_h \leq 0.55$.

In conclusion, we have demonstrated that the A-type AFM $\text{Nd}_{0.45}\text{Sr}_{0.55}\text{MnO}_3$ is metallic below T_N . We suggest that the A-type AFM state with $d_{x^2-y^2}$ -type orbitals near $x \sim 1/2$ forms a new class of layered metallic AFM manganites where the metallic conductivity is mediated by the DE mechanism. Being consistent with our prediction, $\text{Nd}_{0.45}\text{Sr}_{0.55}\text{MnO}_3$ exhibits clear anisotropic spin-wave dis-

persion relations. The transition to the A-type AFM state is, in fact, a spin-lattice coupled transition which is triggered by the orbital ordering, and is considered to be a good example of a phase transition in a multicomponent order-parameter system with spin, lattice, and orbital freedoms. Unlike other charge-ordered manganites, however, the orbital ordering is decoupled from the charge ordering in $\text{Nd}_{0.45}\text{Sr}_{0.55}\text{MnO}_3$. In addition, we demonstrated that the FM spin fluctuation whose energy scale is of order of $\sim 14 \text{ meV \AA}^2$ is dominant in the insulating paramagnetic state.

This work was supported by a Grant-In-Aid for Scientific Research from the Ministry of Education, Science, Sports and Culture, Japan, by Special Researcher's Basic Science Program (RIKEN) and by the New Energy and Industrial Technology Development Organization (NEDO) of Japan. The work at ORNL was supported by U.S. DOE under contract No. DE-AC05-96OR22464 with Lockheed Martin Energy Research Corp., and was carried out under the U.S.-Japan Cooperative Program on Neutron Scattering.

-
- ¹Y. Tomioka *et al.*, J. Phys. Soc. Jpn. **64**, 3626 (1995); Phys. Rev. B **53**, R1689 (1996).
²H. Yoshizawa *et al.*, Phys. Rev. B **52**, R13 145 (1995); J. Phys. Soc. Jpn. **65**, 1043 (1996).
³H. Kuwahara *et al.*, Science **270**, 961 (1995).
⁴H. Kawano *et al.*, Phys. Rev. Lett. **78**, 4253 (1997); Physica B (to be published).
⁵K. Hirota *et al.*, J. Phys. Soc. Jpn. **65**, 3736 (1996); F. Moussa *et al.*, Phys. Rev. B **54**, 15 149 (1996).
⁶R. Kajimoto *et al.*, Physica B (to be published); R. Kajimoto *et al.* (unpublished).

- ⁷W. Bao *et al.*, Phys. Rev. Lett. **78**, 543 (1997).
⁸W. Bao *et al.*, Phys. Rev. Lett. **78**, 507 (1997).
⁹R. Maezono *et al.* (unpublished); T. Mizokawa and A. Fujimori, Phys. Rev. B **56**, R493 (1997); W. Koshibae *et al.*, J. Phys. Soc. Jpn. **66**, 957 (1997).
¹⁰H. Kuwahara, Y. Tomioka, and Y. Tokura (unpublished).
¹¹M. Jaime *et al.*, Phys. Rev. B **54**, 11 914 (1996); B. Fisher *et al.*, *ibid.* **55**, 9227 (1997); T. T. M. Palstra *et al.*, *ibid.* **56**, 5104 (1997).
¹²J. W. Lynn *et al.*, Phys. Rev. Lett. **76**, 4046 (1996).